INTEGRATED SPECTRAL ANALYSIS OF LUNAR SURFACE MINERALOGY.

A. M. Dapremont[1] (Angela.Dapremont@jhuapl.edu) and R. L. Klima[1], [1]Johns Hopkins University Applied Physics Laboratory.

Introduction: Mission objectives of the Korea Pathfinder Lunar Orbiter (KPLO), South Korea's first lunar mission, launched in August of 2022, include: (a) conducting scientific investigations of the lunar environment and (b) identifying future prospective landing sites for lunar missions [1]. The KPLO instrument suite includes a series of cameras to characterize lunar regolith (PolCam), permanently shadowed regions (ShadowCam), and future landing sites (LUTI), as well as a gamma ray spectrometer (KGRS) for mapping of major element distribution [2].

To support these objectives, and augment mission data science potential, we have been working with existing orbital remote sensing datasets to map regional mineral composition. Chandrayaan-1 Moon Mineralogy Mapper (M^3) visible/near-infrared spectrometer [3] and Lunar Prospector (LP) Gamma Ray Spectrometer (GRS) [4] data have been used to investigate a variety of lunar surface terrains to develop a data processing pipeline that will allow for an assessment of combined mineralogical and elemental data variability, and bridge the gap between the relatively low spatial resolution KGRS elemental data and high resolution (< 5 m) LUTI images returned from KPLO.

Methods: M^3 ~1.4 km/pixel parameter maps (e.g., R: IBD1000 G: IBD2000 B: BD1580) were calculated in Environment for Visualizing Images (ENVI) software to identify locations of mineralogical interest, with a particular emphasis on pyroxene-rich deposits, in North Pole, South Pole, and Simple Cylindrical mosaics. LP GRS data were subsequently visualized via the following steps: (1) Planetary Data System (PDS) acquisition of LP GRS elemental abundance data binned at 2 degrees, (2) conversion of GRS elemental weight fractions to raster maps using ArcMap software, and (3) resampling of GRS data to M^3 spatial resolution. These steps were conducted for GRS major oxides, as well as K, Th, and U. Step (3) resampling allowed for simultaneous acquisition of mineralogy and gamma ray spectroscopy data at several pyroxene-rich, Apollo mission landing, and mapped Mare Imbrium lava flow sites of interest. Weight percent (wt %) maps of clinopyroxene, orthopyroxene, iron oxide, olivine, and plagioclase derived from the Kaguya/SELENE Multiband Imager [5] were also resampled to M^3 spatial resolution for mineral abundance.

Pyroxene-rich spectra were modeled using the Modified Gaussian Model (MGM) [6] to derive pyroxene composition for stoichiometry analysis. Contour maps based on GRS elemental data were also created as an additional visualization tool to examine regional elemental abundance ranges.

Results and Discussion: *Mare Imbrium.* The mapped lava flow in the western Mare Imbrium region (~37.79°, -23.27° center) is ~ 2.8E6 km^2. The mapped region average spectrum is consistent with a basaltic composition, with band positions at 1000 nm and 2300 nm (Figure 1c). LP GRS elemental data averaged over the same region suggest that this basalt is relatively high iron, ~ 22 wt % FeO, and low aluminum, ~ 7 wt % Al_2O_3.

Pyroxene Sites. M^3 spectra were acquired from Draper C (~ 17.07°, -21.51°), Epigenes F (~67.11°, -8.12°), and Carlini G (~32.63°, -25.06°) craters. Draper and Epigenes spectra were consistent with clino- and orthopyroxenes, respectively. M^3 spectra showed Carlini G band centers at 970 nm and 2177 nm. 5-band and 7-band MGM fits were modeled, with the latter indicating an average pigeonite (clinopyroxene) or pyroxene mixture composition. Carlini G LP GRS data revealed an abundance of SiO_2 and FeO, while plagioclase and olivine exhibited the highest Kaguya wt % values (Figure 1d).

Apollo Landing Sites. Major elemental oxides from LP GRS and soil compositions of the Apollo missions were most similar at the lunar highlands Apollo 16 landing site, where Mg, Ca, and Ti values exhibited consistency (Figure 1e).

Future Work: Lunar Reconnaissance Orbiter Diviner Lunar Radiometer data will be used to analyze the Christiansen feature position for further compositional constraints. We will also conduct radiative transfer modeling to model mineral abundance in the discussed regions of interest.

Acknowledgments: LP GRS data were acquired from the PDS. We are grateful to NASA for supporting this work through the KPLO Participating Scientist Program. We are also extremely grateful to KARI and the KGRS and LUTI teams for welcoming us onto the team to share in this exciting mission.

References: [1] Korea Pathfinder Lunar Orbiter (KPLO). NASA Space Science Data Coordinated Archive. [2] Korean Pathfinder Lunar Orbiter (KPLO) Status Update. LEAG 2017. [3] Green, R.O., et al. (2011). *JGR, 116*, E00G19. [4] Prettyman, T. H., et al. (2006). *JGR, 111*, E12007. [5] Lemelin, M., et al.

(2015). *JGR, 120*, 869-887. [6] Sunshine, J. M. et al. (1990). *JGR 95*, 6955-6966.

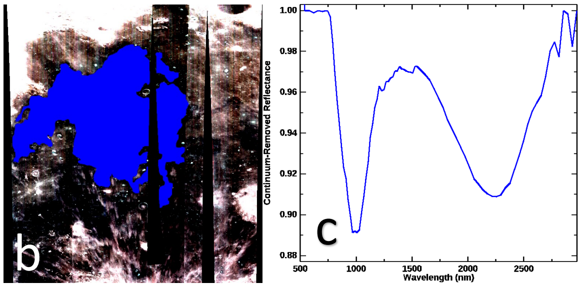

Elemental Oxide	LP GRS %
MgO	7.8
Al_2O_3	7.1
SiO_2	36.3
CaO	11.9
TiO_2	4.9
FeO	21.9

Figure 1. (a) M[3] parameter mosaic with white box denoting general location of mapped Mare Imbrium lava flow in image (b) designated by blue ROI. (c) Average spectrum acquired from ROI of mapped large volcanic region. Table below (b) shows mapped flow LP GRS elemental oxide % values. (d) MGM analysis results for Carlini G crater (~ 4 km in diameter) shown in image inset. Note the Carlini G spectrum denoted by orange symbols and the MGM modeled fit denoted by black spectrum. Left inset table shows LP GRS elemental oxide % values and right inset table shows Kaguya mineral abundance wt % values. (e) Apollo 16 landing site (bland) spectrum with table showing comparison between LP GRS elemental oxide % and lab-measured soil compositions.

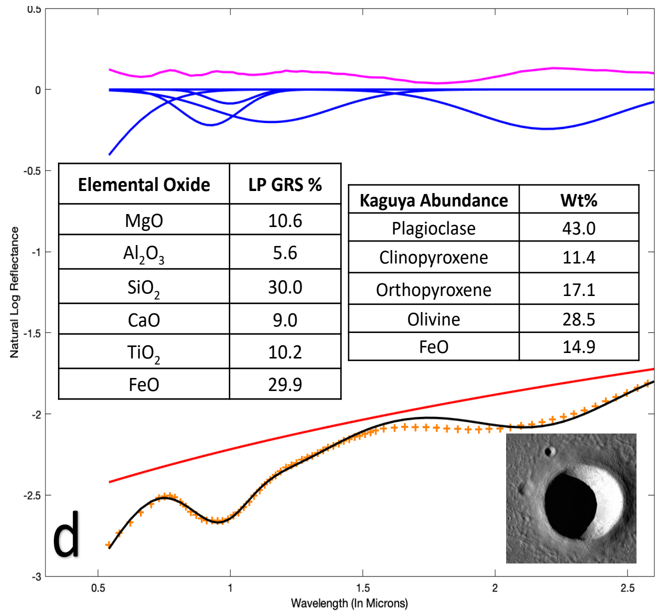

Elemental Oxide	LP GRS %
MgO	10.6
Al_2O_3	5.6
SiO_2	30.0
CaO	9.0
TiO_2	10.2
FeO	29.9

Kaguya Abundance	Wt%
Plagioclase	43.0
Clinopyroxene	11.4
Orthopyroxene	17.1
Olivine	28.5
FeO	14.9

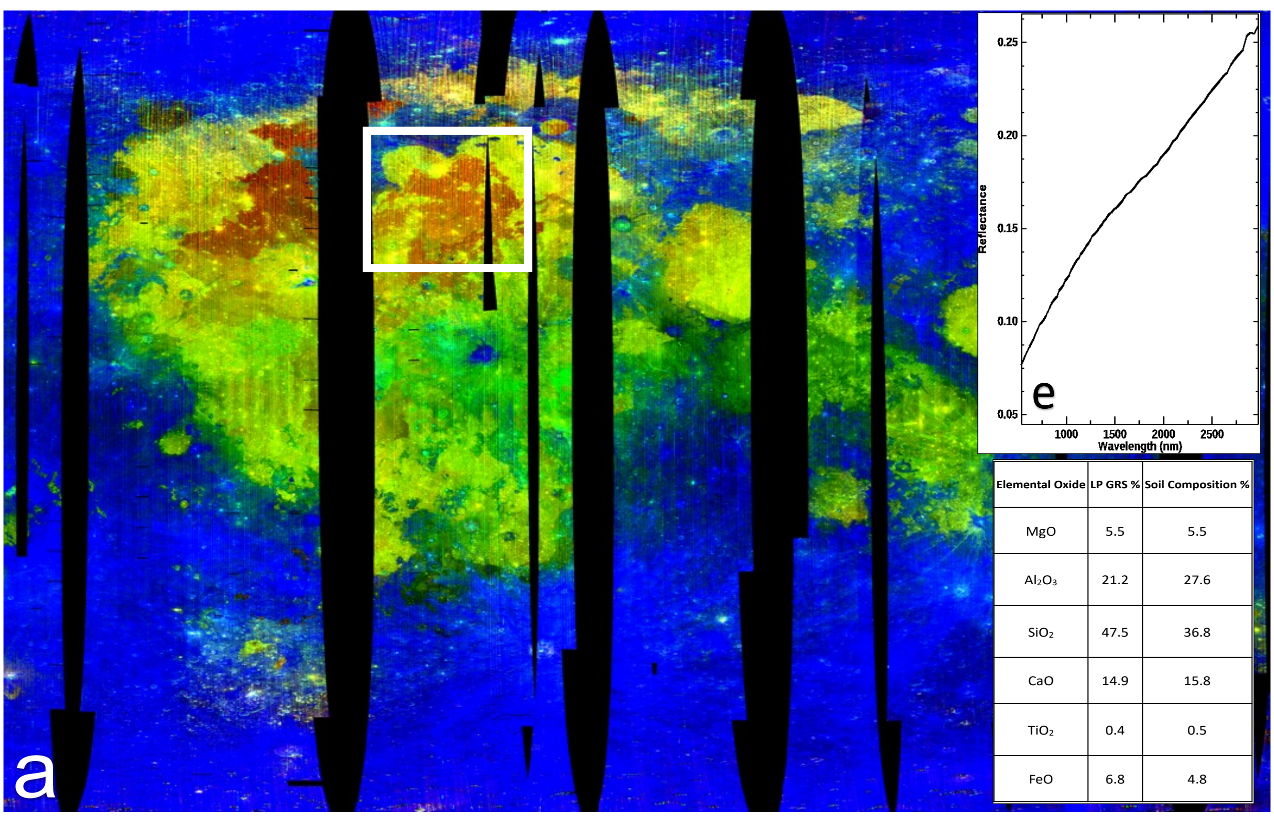

Elemental Oxide	LP GRS %	Soil Composition %
MgO	5.5	5.5
Al_2O_3	21.2	27.6
SiO_2	47.5	36.8
CaO	14.9	15.8
TiO_2	0.4	0.5
FeO	6.8	4.8